

## RESEARCH ARTICLE

# In vivo assignment of methylmalonic acid in breast tissue using 2D MRS and relationship with breast density, menopausal status and cancer risk

Gorane Santamaría<sup>1,2,3</sup>  | Natali Naude<sup>2,3</sup> | Ian Bennett<sup>4,5</sup> | Kirby Vosburgh<sup>5</sup> | Sergi Ganau<sup>6</sup> | Xavier Bargalló<sup>6</sup> | Peter Malycha<sup>2,4,5</sup> | Carolyn Mountford<sup>1,2,5</sup>

<sup>1</sup>Department of Radiology, Princess Alexandra Hospital, Woolloongabba, Queensland, Australia

<sup>2</sup>Translational Research Institute, Woolloongabba, Queensland, Australia

<sup>3</sup>School of Biomedical Sciences, Faculty of Health, Queensland University of Technology, Brisbane City, Queensland, Australia

<sup>4</sup>Department of Breast and Endocrine Surgery, Princess Alexandra Hospital, Woolloongabba, Queensland, Australia

<sup>5</sup>Institute for Glycomics, Gold Coast Campus, Griffith University, Southport, Queensland, Australia

<sup>6</sup>Department of Radiology, Hospital Clinic de Barcelona, Barcelona, Spain

## Correspondence

Gorane Santamaría, Department of Radiology, Princess Alexandra Hospital, 199 Ipswich Rd, Woolloongabba, 4102 QLD, Australia.  
Email: [goranes@gmail.com](mailto:goranes@gmail.com)

## Funding information

This study was supported by the Advance Queensland Initiative, Queensland Government, Australia.

**Background:** Methylmalonic acid (MMA) is linked to progression and aggressiveness of tumours. A recent study showed that high levels of circulatory MMA directed genetic programs promoting cancer progression.

**Purpose:** To evaluate in vivo two-dimensional correlated spectroscopy (2D COSY) data from women at elevated risk of breast cancer to determine if resonances consistent with MMA are present, and if so to correlate levels with breast density, menopausal status and risk categories.

**Materials and methods:** With institutional review board approval, 106 women at elevated risk (mean age 47), including 46 participants at medium risk, 43 at high risk with no known mutation and 17 *BRCA*-mutation carriers, were recruited. Breast density was assessed using a  $T_2$  sequence. A  $T_1$  sequence was used to place the voxel for the 2D COSY data. Peak volumes were normalized to the methylene peak at (1.30, 1.30) ppm. Chi-squared and Mann-Whitney tests were used.

**Results:** Two resonances are assigned on the diagonal at 3.15 ppm and 3.19 ppm consistent with and denoted MMA1 and MMA2 respectively. MMA1 and MMA2 increased in parallel with increased risk. *BRCA*-mutation carriers recorded an increase in mean MMA1 of 120% ( $p = 0.033$ ) and MMA2 of 127% ( $p = 0.020$ ) in comparison with participants with no known mutation. *BRCA*-mutation carriers with dense breasts recorded a significant increase in mean MMA1 of 137% ( $p = 0.002$ ) and in mean MMA2 of 143% ( $p = 0.004$ ) compared with *BRCA*-mutation participants with

**Abbreviations:** 2D COSY, two-dimensional correlated spectroscopy; BI-RADS, Breast Imaging Reporting and Data System; BMI, body mass index; EMT, epithelial-mesenchymal transition; FOV, field of view; HCB, Hospital Clinic de Barcelona, Barcelona, Spain; LDLR, low-density lipoprotein receptor; MMA, methylmalonic acid; NICE, National Institute for Health and Care Excellence; PAH, Princess Alexandra Hospital, Brisbane, Australia; SD, standard deviation; STA, St Andrew's Hospital, Adelaide, Australia;  $T_E$ , echo time;  $T_R$ , repetition time.

This is an open access article under the terms of the [Creative Commons Attribution-NonCommercial-NoDerivs](https://creativecommons.org/licenses/by-nc-nd/4.0/) License, which permits use and distribution in any medium, provided the original work is properly cited, the use is non-commercial and no modifications or adaptations are made.

© 2022 The Authors. *NMR in Biomedicine* published by John Wiley & Sons Ltd.

low-density breast tissue. MMA1 and MMA2 were higher in premenopausal women with dense breasts compared with those with low-density tissue. The highest values of MMA were recorded in *BRCA*-mutation carriers.

**Conclusion:** Two tentative assignments are made for MMA in breast tissue of women at elevated risk for cancer. *BRCA*-mutation carriers exhibited higher values of MMA than those with no known mutation. Premenopausal women with *BRCA* mutation and dense breasts recorded the highest levels of MMA compared with other categories.

#### KEYWORDS

breast density, in vivo MRS, methylmalonic acid, postmenopause, premenopause

## 1 | INTRODUCTION

Methylmalonic acid (MMA),  $\text{CH}_3\text{-CH-(CO}_2\text{H)}_2$ , is a dicarboxylic acid that is a C-methylated derivative of malonate. A recent article has linked increase in MMA with age and a systemic environment that favours the progression and aggressiveness of tumours.<sup>1</sup> The report suggests that MMA in the sera of the aged population is upregulated and induces a complete pro-aggressive epithelial-mesenchymal transition (EMT)-like phenotype in human cancer cell cultures.<sup>1</sup> Specifically, it demonstrates that MMA could induce the human transcription factor SOX4 expression and, consequently, elicit transcriptional reprogramming to give cancer cells aggressive properties. They also hypothesize that MMA may provide a therapeutic target.

Epidemiological studies report breast density to be an independent risk factor for breast cancer<sup>2-4</sup> and to make a woman four to six times more likely to develop breast cancer.<sup>5</sup> Moreover, it has been shown that baseline dense breasts and their persistence over time are strongly associated with an increased risk of incident breast cancer in both premenopausal and postmenopausal women.<sup>6</sup> Additionally, mammographic density has been reported to be under strong genetic influence that may partially explain the familial aggregation of breast.<sup>7</sup> By 2020, 38 states in the United States had notification laws in effect to ensure the patient was notified of her breast density,<sup>8</sup> even though the understanding of cellular and molecular mechanisms underlying the risk of breast cancer had not been determined.

When evaluated with MRI, breast density can be reported using a comparable Breast Imaging Reporting and Data System (BI-RADS).<sup>9</sup> It has recently been reported that there is a significant correlation between breast tissue chemical composition using in vivo two-dimensional correlated spectroscopy (2D COSY) and the breast density as recorded with BI-RADS.<sup>10</sup> The authors reported a gradual increase in the neutral lipid (triglycerides and cholesterol) and metabolite contents from low-density to high-density breasts.

As a consequence of these reports, we explored if any of the unassigned resonances in the in vivo MR spectra of healthy breast tissue were consistent with MMA. Others had assigned MMA in cerebrospinal fluid in a patient with vitamin B<sub>12</sub> deficiency.<sup>11</sup> They demonstrated the pH sensitivity of MMA and reported that the proton MR spectrum of MMA had two multiplets, centred at 1.23 and 3.17 ppm, when recorded in D<sub>2</sub>O at 25 °C and pH 7.2. The multiplets centred at 3.17 ppm had four resonances at 3.14, 3.16, 3.17 and 3.18 ppm in the ratio of 1:4:4:1.

With this information, we hypothesize that MMA can be identified in vivo in the breast tissue using 2D COSY and that levels of MMA are associated with breast density, menopausal status and risk of breast cancer. We aim to evaluate 2D COSY data from women at elevated risk of breast cancer to assign in vivo MMA in the breast tissue, and to correlate MMA levels with breast density, menopausal status and levels of risk.

## 2 | MATERIALS AND METHODS

### 2.1 | Research guidelines and regulations

This cross-sectional study with prospective data collection was undertaken with patients recruited from three hospitals: Princess Alexandra Hospital (PAH), Brisbane, Australia; Hospital Clínic de Barcelona (HCB), Barcelona, Spain; St Andrew's Hospital (STA), Adelaide, Australia. Ethics approval was obtained from all the centres. All research was performed in accordance with relevant guidelines and regulations. Written informed consent was obtained from all participants.

## 2.2 | Inclusion and exclusion criteria

One hundred and six women at elevated risk for breast cancer were recruited. Table 1 shows the sites of recruitment and number of participants at each centre. The mean age was 47 years (standard deviation (SD), 11 years; range, 21–79).

The triage for the elevated risk participants was based on the National Institute for Health and Care Excellence (NICE) guidelines, which classify patients into low (<17%), medium ( $\geq 17\%$  and <30%), or high risk ( $\geq 30\%$ ) depending on the number of family members with breast cancer and their age at diagnosis.<sup>12</sup> Our series included 46 participants at medium risk and 60 at high risk, of whom 43 had no known mutation and 17 were BRCA-mutation carriers.

Fifty-two participants from this series have been reported in a previous study, where four distinct chemical profiles were identified in healthy breast tissue based on breast density and menopausal status in participants at low and high risk with no known mutation.<sup>10</sup>

Participants were excluded if they had breast implants, were claustrophobic, pregnant or breastfeeding or were unable to receive contrast, due to either a known allergy or renal insufficiency.

## 2.3 | MRI

The participants underwent dynamic MRI of the breast and in vivo MR 2D COSY between days 6 and 14 (follicular phase) of the menstrual cycle, where relevant. The data were collected on a 3 T Prisma (PAH) or a 3 T Vida scanner (HCB, STA) (Siemens, Erlangen, Germany) using either an 18-channel (Siemens, Erlangen, Germany) or a 16-channel (RAPID Biomedical, Rimpf, Germany) breast coil (Table 1).

Breast MRI consisted of (a) a localizer sequence (repetition time ( $T_R$ ) 6 ms, echo time ( $T_E$ ) 2.61 ms, slice thickness 7 mm, field of view (FOV)  $400 \times 400 \text{ mm}^2$ ); (b) axial  $T_1$ -weighted 3D FLASH ( $T_R$  5.43 ms,  $T_E$  2.46 ms, flip angle  $20^\circ$ , slice thickness 2 mm, FOV  $320 \times 320 \text{ mm}^2$ , matrix  $448 \times 448 \text{ mm}^2$ ); (c) an axial  $T_2$ -weighted TSE sequence ( $T_R$  4280 ms,  $T_E$  97 ms, slice thickness 2 mm, FOV  $300 \times 300 \text{ mm}^2$ , matrix  $448 \times 448 \text{ mm}^2$ ) and (d) an dynamic axial 3D fat suppressed  $T_1$ -weighted gradient-echo sequence ( $T_R$  4.51 ms,  $T_E$  2.03 ms, flip angle  $10^\circ$ , slice thickness 1.2 mm, FOV  $320 \times 320 \text{ mm}^2$ , matrix  $448 \times 448$ , in-plane resolution  $0.7 \times 0.7 \text{ mm}^2$ , acquisition time 91.5 s). Images were obtained prior to a rapid bolus injection and five times after injection of contrast material. The bolus injection consisted of 0.1 mmol gadobutrol (Gadovist; Bayer, Berlin, Germany) per kilogram of body weight and a 20 mL saline flush, delivered through an intravenous cannula. Automated subtraction of the appropriate precontrast and postcontrast images and multiplanar reconstruction of data sets were performed.

One radiologist undertook the BI-RADS assessment of breast density using the  $T_2$ -weighted sequence. Breast density categories were Type a (fatty breast tissue), Type b (scattered areas of fibroglandular density), Type c (heterogeneous density) and Type d (extremely dense breast tissue). For analysis purposes, the low-density group comprised Type a and Type b and the high-density group was made up of Type c and Type d.

## 2.4 | 2D COSY acquisition and data processing parameters

2D COSY was performed following the dynamic MRI study, as neutral gadolinium chelates, e.g., gadobutrol, have been reported to have little or no effect on the amplitude of the choline peak and are recommended in MRS studies of the breast.<sup>13</sup>

A 3D  $T_1$ -weighted sequence was used to position a voxel of  $20 \text{ mm}^3$  in the left breast. Briefly, the voxel was placed in an area representative of the breast density in each patient, as described elsewhere<sup>10</sup> (Figure 1). The para-areolar region, large blood vessels, chest wall and air-skin interfaces were avoided. Localized shimming was performed by automatic adjustment of zeroth- and first-order shim gradients using the Siemens auto-shimming algorithm,<sup>14</sup> followed by manual adjustment of zeroth-order shim gradients to achieve a width of the water peak at half maximum of 65 Hz or less.

**TABLE 1** Description of participants, devices and breast coils according to sites of recruitment

	PAH	HCB	STA
Number of participants	93	9	4
Risk categories	Medium risk ( $n = 43$ ) High risk no mutation ( $n = 41$ ) BRCA mutation ( $n = 9$ )	Medium risk ( $n = 1$ ) BRCA mutation ( $n = 8$ )	Medium risk ( $n = 2$ ) High risk no mutation ( $n = 2$ )
Vendor	Siemens	Siemens	Siemens
Device (3 T)	Prisma	Vida	Vida
Breast coil	16 channel ( $n = 35$ ) 18 channel ( $n = 58$ )	18 channel	18 channel

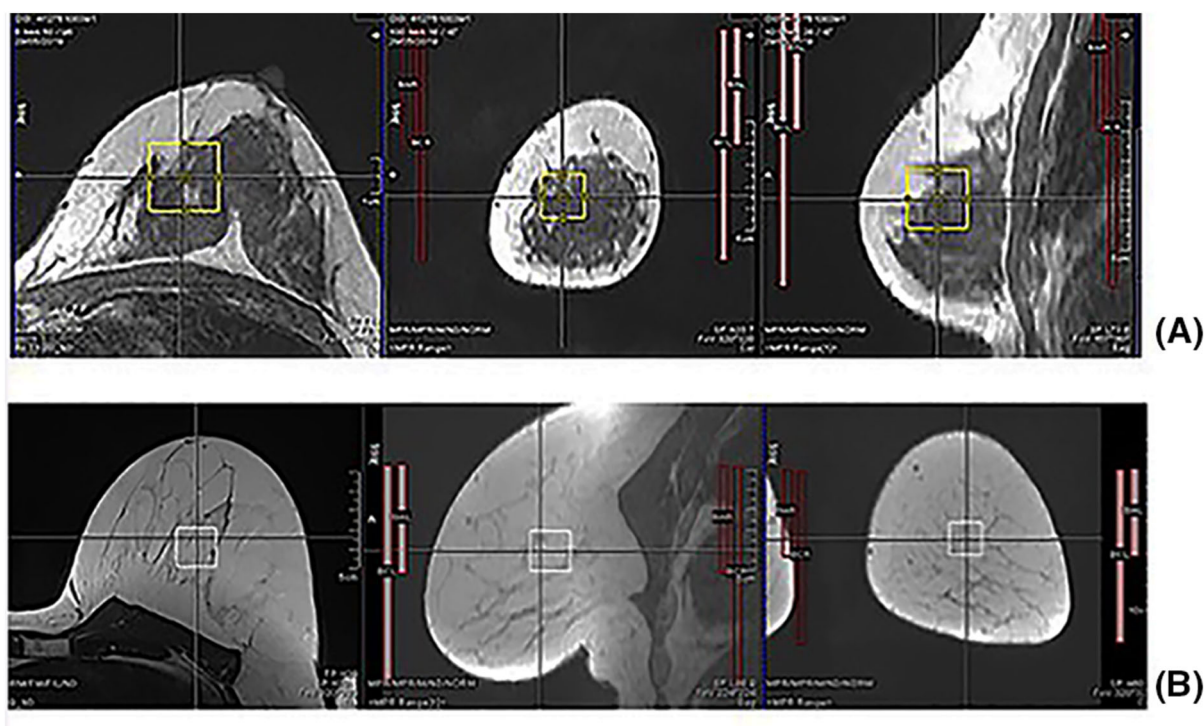


**FIGURE 1** (A), 36-year-old premenopausal woman at high risk with no known mutation. The yellow voxel is placed in the left breast avoiding the chest wall and air or skin interfaces and mainly comprises fibroglandular tissue, as this participant had extremely dense breasts (Type d). (B), 66-year-old postmenopausal woman with *BRCA1* mutation. In this participant with fatty breasts (Type a) the voxel only comprises fatty tissue. Note that the perpendicular lines in the localizer are used for planning the MR sequences. The red boxes on both sides of the images flag the active coils used to record the spectra (left breast in both cases).

Data were acquired using the 2D COSY pulse sequence comprising of three slice-selective pulses ( $90^\circ$ – $180^\circ$ – $90^\circ$ ). The 2D COSY sequence parameters were as follows:  $T_R$  2000 ms,  $T_E$  initial 30 ms, 96  $t_1$  increments at 0.8 ms, six averages per increment,  $f_2$  bandwidth 2000 Hz, vector size 1024 points and RF offset frequency set on 3.2 ppm. Weak water-selective suppression was optimized using the WET technique.<sup>15</sup> The total acquisition time was 19 min.

Processing was undertaken as reported.<sup>16</sup> Briefly, raw data for 2D spectroscopy was processed using MATLAB. Within MATLAB the signal from individual coil elements was combined into a 2D matrix and then reformatted. Each free induction decay (FID) signal was acquired within 1024 points along the directly detected readout dimension— $t_2$ —and 256 increments along the indirectly detected dimension— $t_1$ . The signals were then zero-filled to 2048 and 512 respectively and were then double Fourier transformed ( $F_1 = 1250$  Hz and  $F_2 = 2000$  Hz) after applying temporal filters. A skewed sine-bell squared filter with a skew parameter of 0.3 in the  $t_2$  dimension and a skewed sine-bell filter in the  $t_1$  dimension were applied.<sup>17</sup> Additional processing was undertaken to minimize the lipid contribution by applying a skew parameter of 0.4 in the  $t_2$  dimension where cross-peaks above the diagonal were obscured by  $T_1$  ridges created by methylene.

All diagonal and cross-peak volumes were normalized to the amplitude of the methylene peak at (1.30, 1.30 ppm) as the internal chemical shift reference and measured as described elsewhere.<sup>10</sup> Peak assignments were noted along ( $F_2$ ,  $F_1$ ) in ppm as previously reported in vivo<sup>18</sup> and in breast tissue extracts.<sup>19</sup>

For standard spectral analysis a level multiplier (relating to the number of contour lines) of 1.4 was used in Felix software, whereas for metabolite regions a level multiplier of 1.05 was utilized to make it possible identify the diagonal peaks of metabolites.

Examinations were carried out by experienced radiographers with the assistance of a radiologist, where necessary. All radiographers followed a standard operating procedure to ensure consistent voxel placement, with weekly quality assurance conducted by the lead radiographer to ensure consistency and quality of each acquisition.

## 2.5 | Statistical analysis

Statistical analysis was undertaken using IBM SPSS Statistics 25.0 (IBM, Armonk, NY). Age, body mass index (BMI), MRI-BI-RADS category of breast density, menopausal status, risk group according to NICE guidelines and measured volume of various lipid diagonal peak and cross-peaks, metabolites and cholesterol were collected for each participant.

Chi-squared was used to compare categorical variables. Mean comparison between groups was performed using one-way ANOVA or Kruskal–Wallis non-parametric tests depending upon whether or not the variable followed a normal distribution. A two-sided  $p$  value of less than 0.05 was considered statistically significant.

### 3 | RESULTS

#### 3.1 | Clinical features

The demographics of the series is summarized in Table 2. According to the NICE guidelines, 43% (46/106) of participants were at medium risk and 57% (60/106) at high risk. There were no significant differences across clinical groups in terms of age ( $p = 0.111$ ) or BMI ( $p = 0.633$ ).

Fifty-six percent (59/106) of women had low-density breasts and 44% (47/106) had dense breast tissue ( $p = 0.436$ ).

Forty-three percent (46/106) of the participants were premenopausal and 57% (60/106) had postmenopausal status ( $p = 0.161$ ). In the low-density group 69% (41/59) were postmenopausal, whereas in the high-density group 40% (19/47) were postmenopausal ( $p = 0.003$ ).

#### 3.2 | Chemical evaluation of tissue chemistry

No significant differences were noted between 16- and 18-channel coils in terms of quality and metabolite quantification.

Figure 2 shows a typical 2D COSY spectrum from a premenopausal participant with high-density breasts. A 2D contour plot of the expanded region  $F_2/F_1$  3.00 ppm to 3.80 ppm is shown in Figure 3. The resonances at 3.15 and 3.19 ppm are apparent and consistent with the presence of the MMA molecule in the dense breast tissue (Figure 3). The second multiplet of MMA at 1.23 ppm is not visible due to the large methylene resonance from fatty acyl chains.

#### 3.3 | Relationship of MMA levels with breast density, menopausal status and risk categories

The mean values of MMA1 and MMA2 across risk categories adjusted to breast density are shown in Table 3 and Figure 4.

In the low-density group, MMA1 at 3.15, 3.15 ppm and MMA2 at 3.19, 3.19 ppm average levels did not show significant differences across the risk categories ( $p = 0.193$  and  $p = 0.103$ , respectively).

In the high-density breasts, both MMA1 (3.15, 3.15 ppm) and MMA2 (3.19, 3.19 ppm) displayed significantly different average levels across cohorts ( $p = 0.035$  and  $p = 0.021$ , respectively). The pairwise comparison showed that *BRCA*-mutation carriers had an increase in MMA1 (3.15, 3.15 ppm) of 120% ( $p = 0.033$ ) and in MMA2 (3.19, 3.19 ppm) of 127% ( $p = 0.020$ ) when compared with participants at high risk with no known mutation (Table 3).

*BRCA*-mutation carriers with dense breast tissue recorded a significant increase in MMA1 (3.15, 3.15 ppm) of 137% ( $p = 0.002$ ) and in MMA2 (3.19, 3.19 ppm) of 143% ( $p = 0.004$ ) compared with *BRCA*-mutation participants with low-density breasts (Table 3 and Figure 4).

**TABLE 2** Demographics of the patients included in the series

	Medium risk ( $n = 46$ )	High risk		$P$
		No known mutation ( $n = 43$ )	<i>BRCA</i> mutation ( $n = 17$ )	
Age, mean (SD)	44.8 (12.6)	49.7 (7.6)	45.1 (15.2)	0.111
Menopausal status, %				0.161*
premenopausal	24 (52)	12 (28)	10 (59)	
postmenopausal	22 (48)	31 (72)	7 (41)	
Breast density, %				0.436*
low density	26 (57)	25 (58)	8 (47)	
high density	20 (43)	18 (42)	9 (53)	
BMI, mean (SD)	27.1 (4.9)	27.1 (5.2)	28.5 (7.9)	0.633

\* $p$  value calculated comparing elevated risk participants versus *BRCA*-mutation carriers.

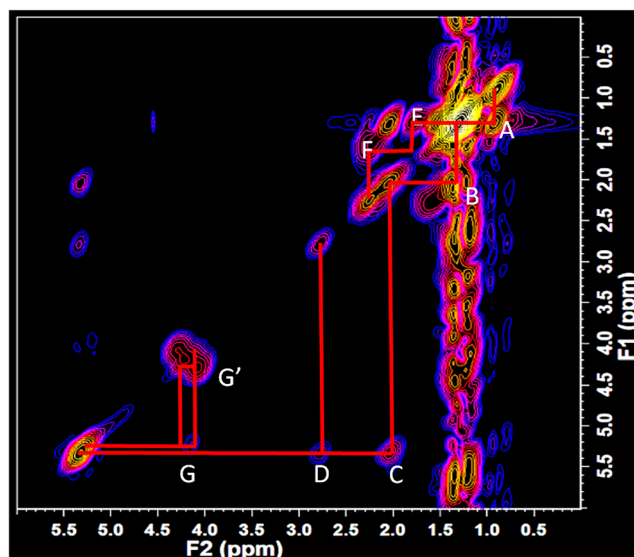


**FIGURE 2** Typical 2D COSY spectrum of the region  $F_2/F_1$  0.00 ppm to 6.00 ppm from the participant in Figure 1A. Data were collected on a Prisma 3 T scanner equipped with a dedicated 18-channel breast coil. The lipids and cross-peaks labelled A–G' are assigned as described by Ramadan et al.<sup>16</sup> Cross-peak A at 0.90, 1.30 ppm,  $(CH_2)_n-CH_2-CH_3$ ; Cross-peak B at 1.30, 2.02 ppm, allylic- $(CH_2)_n$ ; Cross-peak C at 2.02, 5.31 ppm, olefinic-allylic; Cross-peak D at 2.02, 5.31 ppm, olefinic-diallylic; Cross-peak E at 1.59, 1.30 ppm,  $(CH_2)_n-\beta$ -carbonyl; Cross-peak F at 2.25, 1.59 ppm,  $\alpha$ -carbonyl- $\beta$ -carbonyl; Cross-peak G at 4.10, 5.31 ppm, olefinic-glycerol  $(CH_2)$ ; Cross-peak G' at 4.10, 4.25 ppm, glycerol geminal coupling  $(CH_2)$ .

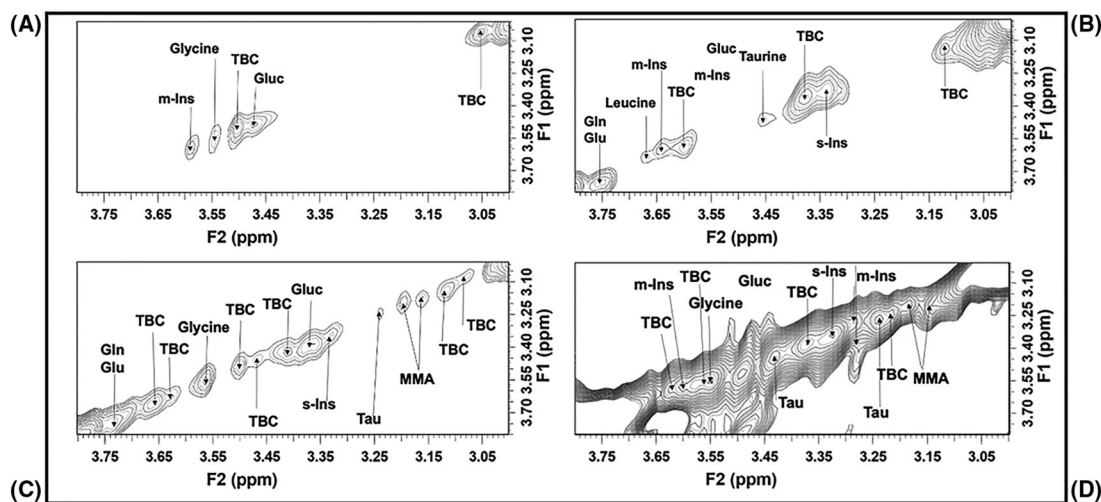


**FIGURE 3** The 2D contour plots from the spectral region  $F_2/F_1$  3.00 ppm to 3.80 ppm (metabolite region). All peak volumes were normalized to the amplitude of the methylene peak at 1.30, 1.30 ppm as the internal chemical shift reference. For this region, a level multiplier of 1.05 was utilized to make it possible to identify the diagonal peaks of metabolites. The MMA molecule is seen as two diagonal peaks making up the multiplets at 3.15 and 3.19 ppm in participants with dense breasts (C and D). A, Premenopausal participant with low-density breast. B, Postmenopausal participant with low-density breast. C, Premenopausal participant with high-density breast. D, Postmenopausal participant with high-density breast. Other diagonal resonances include the following: Gluc, glucose; Gln, glutamine; Glu, glutamate; m-Ins, myo-inositol; s-Ins, scyllo-inositol; Tau, taurine; TBC, to be confirmed.

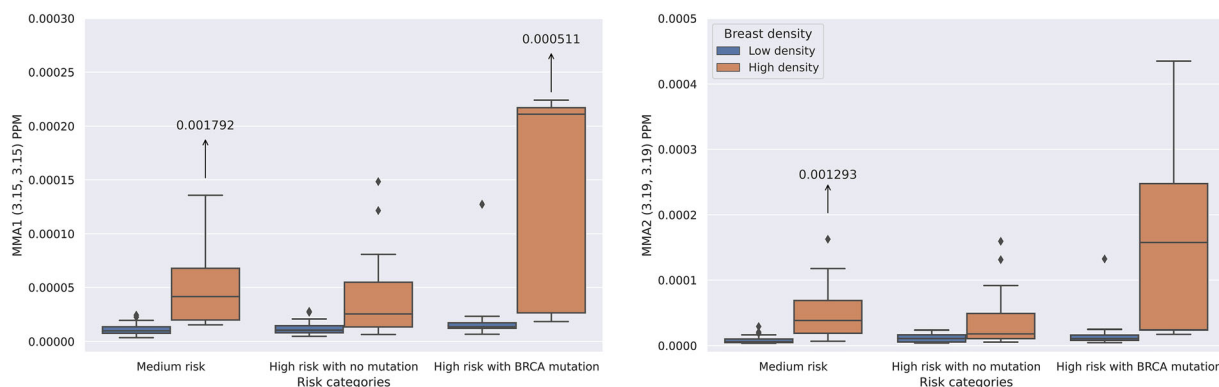
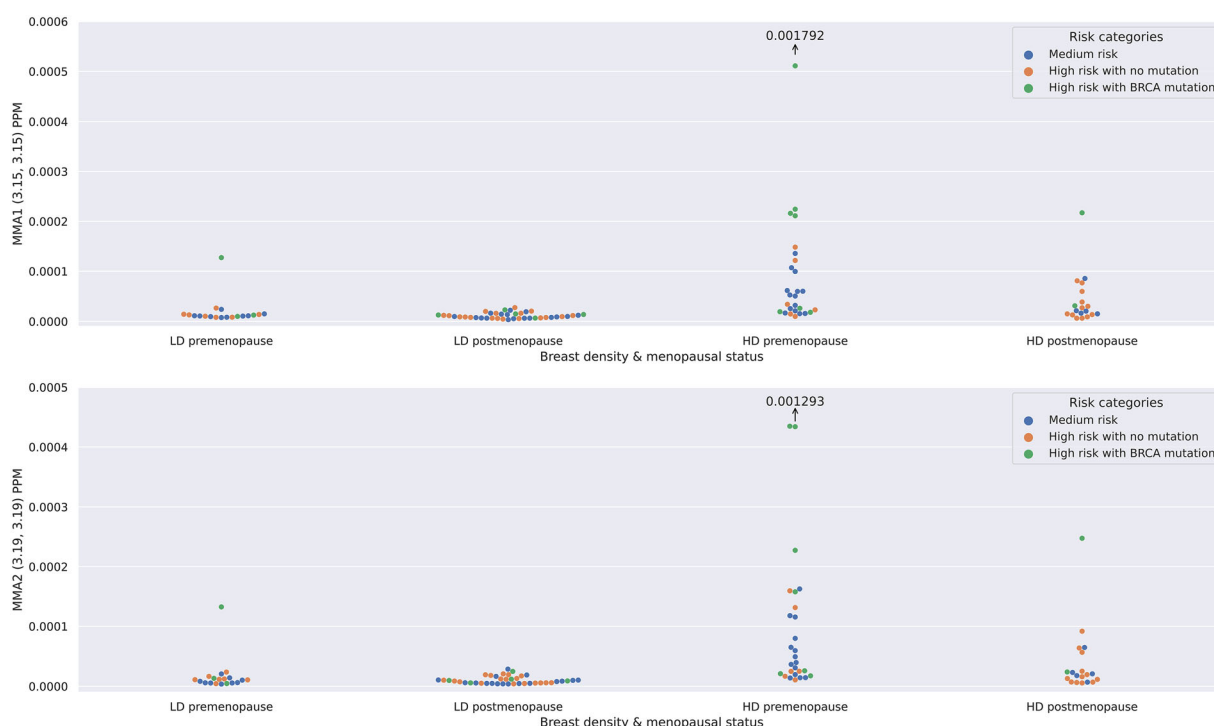
The peak volumes assigned to MMA in each patient categorized by breast density and menopausal status are presented in Figure 5. Both MMA1 (3.15, 3.15 ppm) and MMA2 (3.19, 3.19 ppm) had higher values in premenopausal women with dense breast tissue. In addition, the highest values in this category were recorded in BRCA-mutation carriers.

Participants with low-density breasts, regardless of the risk category, recorded the lowest levels of both molecules of MMA (Figure 5).

**TABLE 3** Mean (SD) of MMA1 (3.15, 3.15 ppm) and MMA2 (3.19, 3.19 ppm) across the risk categories adjusted to breast density

	Low density ( <i>n</i> = 59)				High density ( <i>n</i> = 47)			
	Medium risk	High risk with no mutation	High risk with <i>BRCA</i> mutation	<i>p</i>	Medium risk	High risk with no mutation	High risk with <i>BRCA</i> mutation	<i>p</i>
MMA1 (3.15, 3.15 ppm)	1.1 (0.5)	1.2 (0.6)	2.8 (4.1)	0.193	13.5 (39.2)	4.1 (4.1)	16.4 (16.2)	0.035
MMA2 (3.19, 3.19 ppm)	0.9 (0.6)	1.1 (0.6)	2.6 (4.3)	0.103	11.2 (28.1)	3.8 (4.6)	17.7 (17.2)	0.021

Numbers written in scientific notation ( $\times 10^{-5}$ ).

**FIGURE 4** Box plots show median values and interquartile range of MMA1 at 3.15, 3.15 ppm (left) and MMA2 at 3.19, 3.19 ppm (right) across the risk categories grouped by breast density type. *BRCA*-mutation carriers with high-density breasts exhibit the highest volumes of these molecules. Arrows at the top of the medium-risk and high-risk with *BRCA* mutation box plots on the left mean that there are further values at 0.001792 and at 0.000511, respectively. The same applies in the box plot on the right.**FIGURE 5** The dot plots show a comparison of the resonance volumes recorded for MMA1 (3.15, 3.15 ppm) (top) and MMA2 (3.19, 3.19 ppm) (bottom) across categories combining breast density and menopausal status. Overall, premenopausal women with high-density breasts exhibited higher values of both molecules in comparison with other categories. Each participant is coded according to the risk categories. Arrows at the top of the high-density premenopause plots mean there are further values at 0.001792 (top) and at 0.001293 (bottom).

## 4 | DISCUSSION

We have tentatively assigned MMA in healthy breast tissue in a cohort of participants at elevated risk of developing breast cancer using 2D COSY in a clinical 3 T MR scanner. The methods described here for the in vivo assignment of MMA in breast tissues may provide an important clue, particularly since the highest levels of this molecule were recorded in *BRCA*-mutation carriers with premenopausal status and dense breasts.

Why women with dense breast tissue have an elevated risk of breast cancer has remained largely unexplained. Currently, there is no clinical technique to distinguish individual women at a higher risk. Breast density, and its changes over time, were found to be independently associated with the risk of breast cancer in both premenopausal and postmenopausal women.<sup>6</sup> Importantly, it has been reported that breast cancer risk decreases as density regresses.<sup>6</sup>

MMA is a vital intermediate in the metabolism of fat and protein and is widely known to be a marker of vitamin B<sub>12</sub> deficiency.<sup>20</sup> Recently, MMA has been shown to be associated with the capacity to endow cancer cells with the properties necessary to migrate, invade, survive and thrive as metastatic lesions.<sup>1</sup> Gomes et al. suggest that MMA relies on the activation of the transforming growth factor  $\beta$  (TGF $\beta$ ) signalling in an autocrine fashion to induce SOX4 and, consequently, the transcriptional reprogramming necessary for the EMT that sustains tumour progression.<sup>1,21</sup>

A recent paper has used an integrative genomic strategy to detect regulators of low-density lipoprotein receptor (LDLR) activity.<sup>22</sup> They demonstrated that MMA upregulates LDLR activity by inhibiting 3-hydroxy3-methylglutaryl coenzyme A reductase activity and reducing cholesterol biosynthesis. This suggests that MMA may be a controlling factor in cholesterol homeostasis and may play a role in breast density and cancer risk.

If the assignment of MMA in the breast tissue is correct, then this may provide insight into why, in a cohort of individuals at elevated risk, premenopausal women with *BRCA* mutation and dense breasts have even a higher risk for developing breast cancer. It is also of interest to note that those individuals with low-density breasts exhibited much lower volumes of MMA1 and MMA2, regardless of the risk category and menopausal status. According to our results, MMA appears to be related to breast density, which is one of the known risk factors for breast cancer. The fact that MMA enables cells to acquire pro-aggressive traits and is involved in tumour development suggests that this molecule could potentially be a biomarker of breast cancer.

The capacity to non-invasively monitor breast tissue chemistry changes at a molecular level in a healthy breast, using in vivo 2D COSY in a clinical MR scanner, shows great potential for the development of a personalized medicine approach. This is particularly relevant in the cohort of women with a germline *BRCA* mutation or with familial history with no known mutation, as it is widely known that these women are at higher risk of breast cancer and are diagnosed and die at earlier ages than the general population.<sup>23,24</sup> The current results obtained from a series at elevated risk including *BRCA*-mutation carriers are in line with those reported in a previous study, in which women at high risk with no known mutation exhibited the highest lipid content and metabolic activity in the high-density premenopausal category when compared with women at low risk, who exhibited the highest metabolic activity in the high-density postmenopausal category.<sup>10</sup>

There are some limitations of the study. First, the number of *BRCA*-mutation carriers was smaller than those of the other risk categories, which may impact the results. Second, although this is a multicentric study, most of the participants were recruited at one hospital (PAH). However, the results consistently show that premenopausal women with dense breast exhibit higher levels of MMA, regardless of the site of recruitment. Third, the breast density assessment was performed by one radiologist, so interobserver variability could not be evaluated.

In conclusion, a new molecule, MMA, is tentatively assigned in the in vivo 2D COSY recorded in breast tissue of healthy women at elevated risk of breast cancer. *BRCA*-mutation carriers exhibited higher values of MMA than those with no known mutation, and premenopausal women with *BRCA* mutation and dense breasts showed the highest levels of MMA when compared both with postmenopausal participants with *BRCA* mutation and dense breasts, and with those with low-density breasts regardless of their menopausal status or risk categories.

If confirmed in larger samples, we consider these in vivo MMA assignments in the breast tissue to be an important finding, as this could provide an early warning of developing breast cancer. These findings make it important to evaluate the MMA levels in the breast tissues of healthy women and those with a breast cancer to gain further understanding of the role of this molecule in tumour development and progression.

### 4.1 | Data collection and expertise required

The clinical study reported here was established in Brisbane at a public hospital with a senior radiographer (Tech) operating the scanner. This knowledge was transferred to radiographers in a private practice in Adelaide and then to a major public hospital in Barcelona. The original radiographers monitored data quality from each site. The data as currently analysed requires knowledge of 2D COSY, but we are in the process of automating the data evaluation and plan for it to be cloud based in collaboration with two commercial partners.

## ACKNOWLEDGEMENTS

The authors thank Timothy King and Jillian Borthwick from STA for their assistance in participant recruitment and data acquisition, Darren Lukas for assistance with the figures and John Irvine for assistance in statistical analysis. Open access publishing facilitated by Queensland University of Technology, as part of the Wiley - Queensland University of Technology agreement via the Council of Australian University Librarians.

## ORCID

Gorane Santamaría  <https://orcid.org/0000-0001-5915-8580>

## REFERENCES

- Gomes AP, Ilter D, Low V, et al. Age-induced accumulation of methylmalonic acid promotes tumour progression. *Nature*. 2020;585(7824):283-287. doi:10.1038/s41586-020-2630-0
- McCormack VA, dos Santos SI. Breast density and parenchymal patterns as markers of breast cancer risk: a meta-analysis. *Cancer Epidemiol Biomarkers Prev*. 2006;15(6):1159-1169. doi:10.1158/1055-9965.EPI-06-0034
- Boyd NF, Lockwood GA, Byng JW, Tritchler DL, Yaffe MJ. Mammographic densities and breast cancer risk. *Cancer Epidemiol Biomarkers Prev*. 1998;7(3/4):1133-1144. doi:10.3233/BD-1998-103-412
- Duffy SW, Morrish OWE, Allgood PC, et al. Mammographic density and breast cancer risk in breast screening assessment cases and women with a family history of breast cancer. *Eur J Cancer*. 2018;88:48-56. doi:10.1016/j.ejca.2017.10.022
- Boyd NF, Guo H, Martin LJ, et al. Mammographic density and the risk and detection of breast cancer. *N Engl J Med*. 2007;356(3):227-236. doi:10.1056/NEJMoa062790
- Kim EY, Chang Y, Ahn J, et al. Mammographic breast density, its changes, and breast cancer risk in premenopausal and postmenopausal women. *Cancer*. 2020;126(21):4687-4696. doi:10.1002/cncr.33138
- Brand JS, Humphreys K, Thompson DJ, et al. Volumetric mammographic density: heritability and association with breast cancer susceptibility loci. *J Natl Cancer Inst*. 2014;106(12):dju334. doi:10.1093/jnci/dju334
- Kyanko KA, Hoag J, Busch SH, et al. Dense breast notification laws, education, and women's awareness and knowledge of breast density: a nationally representative survey. *J Gen Intern Med*. 2020;35(7):1940-1945. doi:10.1007/s11606-019-05590-7
- D'Orsi CJ, Sickles EA, Mendelson E, et al. *ACR BI-RADS Atlas, Breast Imaging Reporting and Data System*. American College of Radiology; 2003.
- Santamaría G, Naude N, et al. Breast tissue chemistry measured in vivo in healthy women correlate with breast density and breast cancer risk. *J Magn Reson Imaging*. 2022;56(5):1355-1369. doi:10.1002/jmri.28168
- Commodari F, Arnold DL, Sanctuary BC, Shoubridge EA. <sup>1</sup>H NMR characterization of normal human cerebrospinal fluid and the detection of methylmalonic acid in a vitamin B<sub>12</sub> deficient patient. *NMR Biomed*. 1991;4(4):192-200. doi:10.1002/nbm.1940040407
- Mulsow J, Lee J, Dempsey C, Rithwell J, Geraghty JG. Establishing a family risk assessment clinic for breast cancer. *Breast J*. 2009;15(Suppl 1):S33-S38. doi:10.1111/j.1524-4741.2009.00825.x
- Lenkinski RE, Wang X, Elian M, Golberg SN. Interaction of gadolinium-based MR contrast agents with choline: implications for MR spectroscopy (MRS) of the breast. *Magn Reson Med*. 2009;61(6):1286-1292. doi:10.1002/mrm.21937
- Mountford C, Ramadan S, Stanwell P, Malycha P. Proton MRS of the breast in the clinical setting. *NMR Biomed*. 2009;22(1):54-64. doi:10.1002/nbm.1301
- Ogg RJ, Kingsley PB, Taylor JS. WET, a T<sub>1</sub>- and B<sub>1</sub>-insensitive water-suppression method for in vivo localized <sup>1</sup>H NMR spectroscopy. *J Magn Reson*. 1994;104(1):1-10. doi:10.1006/jmrb.1994.1048
- Ramadan S, Arm J, Silcock J, et al. Lipid and metabolite deregulation in the breast tissue of women carrying BRCA1 and BRCA2 genetic mutations. *Radiology*. 2015;275(3):675-682. doi:10.1148/radiol.15140967
- Delikatny EJ, Hull WE, Mountford CE. The effect of altering time domains and window functions in two-dimensional proton COSY spectra of biological specimens. *J Magn Reson*. 1991;94(3):563-573. doi:10.1016/0022-2364(91)90143-H
- Thomas MA, Lipnick S, Velan S, et al. Investigation of breast cancer using two-dimensional MRS. *NMR Biomed*. 2009;22(1):77-91. doi:10.1002/nbm.1310
- Sitter B, Sonnewald U, Spraul M, Fjösne HE, Gribbestad IS. High-resolution magic angle spinning MRS of breast cancer tissue. *NMR Biomed*. 2002;15(5):327-337. doi:10.1002/nbm.775
- Chandler RJ, Venditti CP. Genetic and genomic systems to study methylmalonic acidemia. *Mol Genet Metab*. 2005;86(1/2):34-43. doi:10.1016/j.ymgme.2005.07.020
- Jianchao Z, Quian L, Yang L, et al. SOX4 induces epithelial-mesenchymal transition and contributes to breast cancer progression. *Cancer Res*. 2012;72(17):4597-4608. doi:10.1158/0008-5472.CAN-12-1045
- Goedeke L, Canfrán-Duque A, Rotllan N, et al. MMAB promotes negative feedback control of cholesterol homeostasis. *Nat Commun*. 2021;12(1):6448. doi:10.1038/s41467-021-26787-7
- Collins JM, Isaacs C. Management of breast cancer risk in BRCA1/2 mutation carriers who are unaffected with cancer. *Breast J*. 2020;26(8):1520-1527. doi:10.1111/tbj.13970
- Brandt A, Bermejo JL, Sundquist J, Hemminki K. Age of onset in familial breast cancer as background data for medical surveillance. *Br J Cancer*. 2010;102(1):42-47. doi:10.1038/sj.bjc.6605421

**How to cite this article:** Santamaría G, Naude N, Bennett I, et al. In vivo assignment of methylmalonic acid in breast tissue using 2D MRS and relationship with breast density, menopausal status and cancer risk. *NMR in Biomedicine*. 2022;e4851. doi:10.1002/nbm.4851